Available online at www.sciencedirect.com
SCIENCE DIRECT
Catalysis Today 116 (2006) 377–383
CATALYSIS TODAY
www.elsevier.com/locate/cattod

A comparative study of catalysts for the preferential CO oxidation in excess hydrogen

Eun-Yong Ko [a], Eun Duck Park [a,*], Kyung Won Seo [a], Hyun Chul Lee [b], Doohwan Lee [b], Soonho Kim [b]

[a] *Department of Chemical Engineering, Division of Chemical Engineering and Materials Engineering, Ajou University, Wonchun-Dong, Yeongtong-Gu, Suwon 443-749, Republic of Korea*
[b] *Energy Laboratory, Samsung Advanced Institute of Technology (SAIT), P.O. Box 111, Suwon 440-600, Republic of Korea*

Available online 5 July 2006

Abstract

Selective CO oxidation in the presence of excess hydrogen was studied over metal oxides (CoO and CuO–CeO_2), supported gold catalysts (Au/γ-Al_2O_3, Au/CuO, Au/CeO_2/γ-Al_2O_3, Au/CuO–CeO_2 and Au/CeO_2), and supported Pt catalysts (Pt/γ-Al_2O_3, Pt–Ni/γ-Al_2O_3, and Pt–Co/γ-Al_2O_3). The methanation was dominant over CoO in the presence of excess H_2. CuO–CeO_2 was quite selective for CO oxidation at low temperatures. However, the presence of CO_2 and H_2O retarded its catalytic activity. No beneficial effect to CO_2 selectivity was observed when Pt, Ru, Ni, and Co was added to CuO–CeO_2 as a modifier. Supported gold catalysts showed the high CO conversion at low temperatures. However, the CO_2 selectivity decreased noticeably with increasing H_2 concentration in a reactant. Pt–Ni/γ-Al_2O_3 showed the highest CO conversion with a high CO_2 selectivity over a wide reaction temperature among above catalysts examined at the same reaction condition. This catalyst also showed the best performance in the presence of 2 vol.% H_2O and 20 vol.% CO_2.

Keywords: CO oxidation; PROX; Pt–Ni/γ-Al_2O_3; Fuel cell; PEMFC

1. Introduction

Reforming of hydrocarbons followed by water–gas shift reaction is commonly used to produce the hydrogen fuel for the polymer electrolyte membrane fuel cell (PEMFC), which has been attracting much attention in the application to electric vehicles or residential power-generations [1]. However, 0.5–1 vol.% of carbon monoxide is usually contained in the hydrogen fuel from the water–gas shift reactor. Because platinum, an anode of PEMFC, is prone to be poisoned in the presence of small amounts of CO in the hydrogen stream, carbon monoxide should be removed to a trace-level. The acceptable CO concentration is below 10 ppm at Pt anode and below 100 ppm at CO-tolerant alloy anodes [2]. Several different methods for the CO removal have been studied including purification with metal membrane [3], selective CO oxidation [2], and CO methanation [4]. Among them, the selective oxidation has been accepted as the most effective way to achieve this goal. In this system, the following three reactions can occur.

$$CO + (1/2)O_2 \rightarrow CO_2 \quad (1)$$

$$H_2 + (1/2)O_2 \rightarrow H_2O \quad (2)$$

$$CO + 3H_2 \rightarrow CH_4 + H_2O \quad (3)$$

The third reaction, which is called methanation, should be avoided except that CO concentration was quite low because it consumed relatively large amounts of hydrogen compared with the preferential CO oxidation (PROX). A number of catalysts more active for the first reaction than the second reaction have been reported [2,5–49]. They can be grouped into metal oxides [5–20], supported gold catalysts [21–29], supported Rh catalysts [30], supported Ru catalysts [31,32], and supported Pt catalysts [32–49]. CoO was reported to show the best performance among 3d transition metal oxides [5]. Among mixed metal oxides, CuO–CeO_2 has been claimed to be quite active and intensively studied by several groups [6–20]. The effect of preparation method [11–13], pretreatment condition

* Corresponding author. Tel.: +82 31 219 2384; fax: +82 31 219 1612.
E-mail address: edpark@ajou.ac.kr (E.D. Park).

0920-5861/$ – see front matter © 2006 Elsevier B.V. All rights reserved.
doi:10.1016/j.cattod.2006.05.072

[14], promoters [15–18], and support [19,20] on the PROX has been reported. For supported gold catalysts, Au/Mn_2O_3 [21], Au/Fe_2O_3 [22,23], $Au/MOx/Al_2O_3$ [24,25], and Au/CeO_2 [26–29] have been reported to be active for the PROX. Supported platinum catalysts have been considered to be promising since the PROX in excess hydrogen stream attracted attention for its practical applications. However, they usually showed noticeable activities only above 423 K [33–35]. Because PEMFC is usually operated below 423 K, catalysts operating at low temperatures can be more plausible. To increase catalytic activities at low temperatures, different methods have been tried for supported platinum catalysts. The pretreatment of Pt catalyst with water vapor was reported to enhance low-temperature catalytic activities for the PROX [36]. Several groups have reported that the PROX at low temperatures could be enhanced by the addition of 2nd metals such as Fe [37–40], Ce [41], Co [42–46], Ni [42,44], Mn [44], and alkali metals [46–49].

Most PROX catalyst was proved its superiority by comparison with a reference catalyst selected by each research group under different reaction conditions. Until now, only limited comparisons among these PROX catalysts have been conducted at the same reaction condition [50]. Recently, we found that supported Pt–Ni and Pt–Co catalysts could be promising PROX catalysts [42,43]. These catalysts were prepared by a co-impregnation method from metal precursors containing no chlorine compounds. In this work, these catalysts were compared with other well-known PROX catalysts under the same reaction condition.

2. Experimental

The cobalt oxide (Co_3O_4) was prepared by a precipitation method. The pH of an aqueous solution of $Co(NO_3)_2$ was increased to 8 by an addition of 1 M NaOH solution. The slurry was aged for 1 h at 353 K, filtered, and washed with de-ionized water several times to remove sodium ion. The cake was then dried at 373 K overnight. Cobalt oxide was reduced with hydrogen at 473 K before a reaction.

The $CuO–CeO_2$ catalyst was prepared by the co-precipitation method. The precursor salts, $Cu(NO_3)_2{\cdot}3H_2O$ and $Ce(NO_3)_3{\cdot}6H_2O$, were dissolved in de-ionized water. One molar of NaOH solution was added to the mixed salt solution under vigorous stirring to precipitate the metals as hydroxides. The pH of the solution was controlled at 8. After aging for 1 h at 353 K, the precipitate was filtered, washed with de-ionized water to remove sodium ion and dried at 373 K overnight. The catalysts were calcined at different temperatures before a reaction. The Cu content of the prepared $CuO–CeO_2$ was intended to be 20 at.%.

The HCl-added $CuO–CeO_2$ catalyst was prepared by a wet impregnation method. The amount of chloride ion was equal to that of copper ion in the $CuO–CeO_2$. This catalyst was calcined in air at 973 K before a reaction. The metal-modified $CuO–CeO_2$ catalysts were also prepared by a wet impregnation method. $Pt(NH_3)_4(NO_3)_2$, H_2PtCl_6, $Ru(NO)(NO_3)_3$, $Ni(NO_3)_2$, and $Co(NO_3)_2$ were utilized as metal precursors. The content of Pt and Ru was designed to be 0.05 wt.%. The content of Ni and Co was intended to be 1 wt.%. These catalysts were calcined in air at 573 K and reduced with H_2 at 573 K before a reaction. The Pt-modified $CuO–CeO_2$ using a Pt precursor such as $Pt(NH_3)_4(NO_3)_2$ and H_2PtCl_6 was denoted as $Pt(N)/CuO–CeO_2$ and $Pt(C)/CuO–CeO_2$, respectively.

$Au/\gamma\text{-}Al_2O_3$, Au/CeO_2-DP, $Au/CeO_2/\gamma\text{-}Al_2O_3$, and $Au/CuO–CeO_2$ were prepared by a deposition–precipitation (DP) method. $\gamma\text{-}Al_2O_3$ was purchased from Alfa and utilized without any further treatment. CeO_2 was prepared by a precipitation method. $CeO_2/\gamma\text{-}Al_2O_3$ was prepared by a wet impregnation method. The content of Ce was intended to be 10 wt.%. This support was calcined in air at 573 K. $CuO–CeO_2$ was calcined in air at 773 K. For the preparation of gold catalysts, these supports were suspended in de-ionized water and the pH of the suspension was preadjusted to 8 with 1 M NaOH solution. An aqueous solution of 0.01 M $AuCl_3$ was subsequently added drop by drop into the slurry, along with a 1.0 M NaOH solution to maintain a pH of 8. After 1 h stirring at 343 K, gold-deposited powders were filtered, washed several times with de-ionized water at room temperature to remove residual chloride ion, dried at 373 K, and stored as a fresh sample. These catalysts were reduced with H_2 at 473 K before a reaction.

Au/CeO_2-CP was prepared by the co-precipitation (CP) method. The precursor salts, $AuCl_3$ and $Ce(NO_3)_3{\cdot}6H_2O$, were dissolved in de-ionized water. One molar of NaOH solution was added to the mixed salt solution with vigorous stirring to precipitate the metals as hydroxides. The pH of the solution was controlled at 8. After aging for 1 h at 353 K, the precipitate was filtered, washed with de-ionized water to remove residual chloride and dried at 373 K overnight. The catalysts were calcined in air at 773 K before a reaction.

Au/CuO was prepared by the deposition–precipitation method from $Cu(OH)_2$. The detailed preparation procedure was same to that of other supported gold catalysts. This catalyst was calcined in air at 573 K before a reaction.

γ-Alumina-supported Pt, Pt–Co, and Pt–Ni catalysts were prepared by a wet impregnation method from an aqueous solution of Pt precursor, $Pt(NH_3)_4(NO_3)_2$, and transition metal precursors, metal nitrates. γ-Alumina (Alfa) was utilized as a support. The content of Pt was 1 wt.% and the molar ratio of Co/Pt and Ni/Pt was 10 and 5, respectively. All the catalysts were calcined in air at 573 K. Before a reaction, $Pt/\gamma\text{-}Al_2O_3$, $Pt–Ni/\gamma\text{-}Al_2O_3$ and $Pt–Co/\gamma\text{-}Al_2O_3$ was reduced with H_2 at 573, 423 and 773 K, respectively.

The gold content was determined by inductively coupled plasma spectrometer (Direct Reading Echelle ICP, LEEMAN ABS. INC., U.S.A.).

Temperature programmed reduction (TPR) was conducted over 0.2 g sample in a 10 vol.% H_2/Ar stream from 313 to 873 K at a heating rate 10 K/min monitoring TCD signals.

Bulk crystalline structures of catalysts were determined with an X-ray diffraction (XRD) technique. XRD patterns were obtained by using Cu Kα radiation using a Rigaku D/MAC-III instrument at room temperature.

The CO chemisorption was conducted over 0.2 g sample in a He stream at 300 K by a pulsed injection of 50 μl of CO after

samples were pretreated sequentially with air and H_2 at designed temperatures for 1 h.

Bright-field images of transmission electron microscopy (TEM) were obtained from a Philips CM 200 TEM operated at 200 kV and used to determine the particle size of gold. Samples were ground in a mortar to fine particles and then dispersed ultrasonically in methanol. The sample was deposited on a Cu grid covered by a holey carbon film.

Reactions were carried out in a small fixed bed reactor with catalysts retained between 45 and 80 mesh sieves. A mixed gas of 1.0 vol.% CO, 1.0 vol.% O_2, 2 vol.% H_2O and 10 (or 80) vol.% H_2 balanced with helium was fed to a reactor at an atmospheric pressure. The catalytic activity was measured from 303 to 573 K at a ramping rate of 1 K/min. The effect of CO_2 was examined with a gas mixture of 1.0 vol.% CO, 1.0 vol.% O_2, 2 vol.% H_2O, 20 vol.% CO_2, and 50 vol.% H_2 balanced with helium. For all experiments, 0.10 g of catalyst without diluents was placed in a reactant gas at a flow rate of 100 ml/min. The effluent from the reactor was analyzed by gas chromatograph (HP5890A, molecular sieve 5A column) to determine CO conversion, O_2 conversion, CO_2 selectivity, and CH_4 yield. The detection limit of CO was 10 ppm. The CO conversion, O_2 conversion, CO_2 selectivity, and the CH_4 yield were calculated using the following formulas:

$$\text{CO conversion}\,(\%) = \{([\text{CO}]_{\text{in}} - [\text{CO}]_{\text{out}})/[\text{CO}]_{\text{in}}\} \times 100;$$

$$\text{O}_2\text{ conversion}\,(\%) = \{([\text{O}_2]_{\text{in}} - [\text{O}_2]_{\text{out}})/[\text{O}_2]_{\text{in}}\} \times 100;$$

$$\text{CO}_2\text{ selectivity}\,(\%) = \{0.5 \times ([\text{CO}]_{\text{in}} - [\text{CO}]_{\text{out}} - [\text{CH}_4]_{\text{out}})/([\text{O}_2]_{\text{in}} - [\text{O}_2]_{\text{out}})\} \times 100;$$

$$\text{CH}_4\text{ yield}\,(\%) = ([\text{CH}_4]_{\text{out}}/[\text{CO}]_{\text{in}}) \times 100.$$

3. Results and discussion

The BET surface areas of Co_3O_4 and CoO prepared by reduction of Co_3O_4 at 473 K with H_2 were determined to be 36 and 87 m^2/g, respectively. Several reduction peaks were observed from Co_3O_4 during TPR experiment; a small reduction peak at 400 K, two large reduction peaks at 480 and 530 K, and a large broad reduction peak from 550 to 770 K. When Co_3O_4 was reduced at 473 K with H_2, the crystalline CoO phase was detected by XRD. This catalyst showed 100% CO conversion at 433 K in the presence of 10% H_2 as shown in Fig. 1. The methanation was observed over this catalyst when the reaction temperature was higher than 473 K. When H_2 concentration increased from 10 to 80%, this methanation occurred at a lower temperature such as 453 K. Furthermore, the CO methanation prevailed over the preferential CO oxidation, which decreased the CO_2 selectivity noticeably when the reaction temperature was above 433 K. Therefore, this CoO catalyst might not be a good candidate for the PROX in the presence of excess H_2.

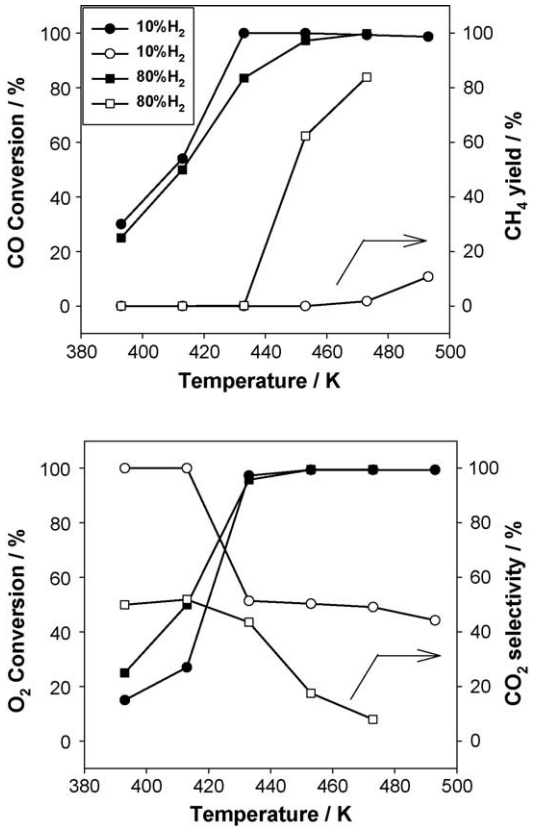

Fig. 1. CO conversion, CH_4 yield, O_2 conversion, and CO_2 selectivity for the PROX over CoO with increasing reaction temperatures. Reactants: 1% CO, 1% O_2, 10% (80%) H_2, and 2% H_2O in He. F/W = 1000 ml/min/g_{cat}.

The PROX of CuO–CeO_2 catalyst was examined in the absence and presence of H_2O as shown in Fig. 2A. This catalyst showed 100% CO conversion from 393 to 443 K in the absence of H_2O. When 2% H_2O was fed with reactants, 100% CO conversion was achieved at higher temperatures of 428–458 K. Only 2% H_2O decreased the low-temperature catalytic activity noticeably. The temperature range showing 100% CO conversion also decreased in the presence of H_2O. This is similar to the previous report that the catalytic activity decreased in the presence of 20% H_2O [8]. The effect of calcination temperature on the PROX in the presence of 80% H_2 was examined as shown in Fig. 2B. The maximum CO conversion was obtained at 393 K irrespective of calcination temperatures. No noticeable difference in CO conversion at temperatures of 393–433 K could be found over CuO–CeO_2 catalysts calcined at different temperatures. When the reaction temperature was higher than 433 K, the CO conversion decreased with increasing calcination temperature. This might be related to the difference in catalytic activity for the water–gas shift reaction. The nano-sized copper oxide on cerium oxide which cannot be stabilized under a high-temperature heat treatment has been reported to be responsible for this reaction [51]. The BET surface area of CuO–CeO_2 calcined with air at 373, 573, 773, and 973 K was determined to be 148, 128, 118, and 50 m^2/g, respectively. XRD also showed that the crystalline size of mixed solution of Cu–Ce–O increased with calcination temperatures.

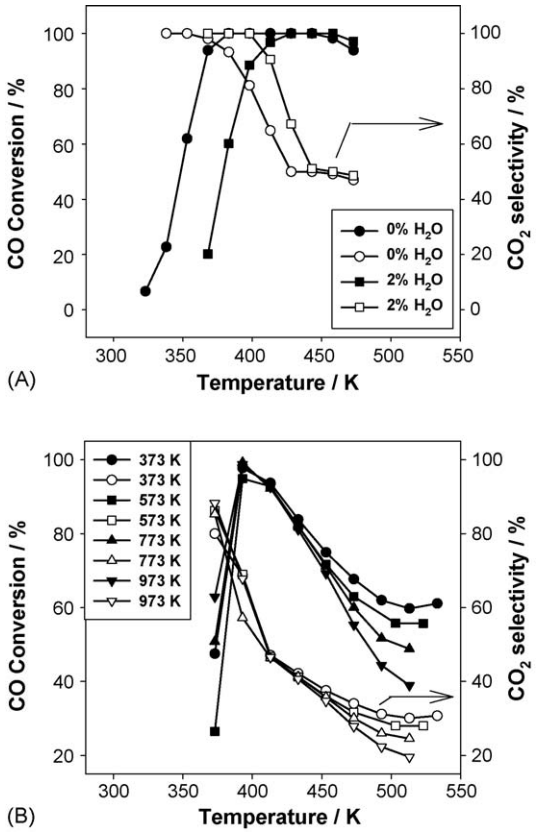

Fig. 2. CO conversion and CO_2 selectivity for the PROX over CuO–CeO_2 containing 20 at.% Cu with increasing reaction temperatures. (A) The catalyst was calcined with air at 573 K; reactants: 1% CO, 1% O_2, and 10% H_2 in He (dry condition); 1% CO, 1% O_2, 10% H_2, and 2% H_2O in He (wet condition). (B) The catalyst was calcined with air at different temperatures; reactants: 1% CO, 1% O_2, 80% H_2, and 2% H_2O in He. F/W = 1000 ml/min/g_{cat}.

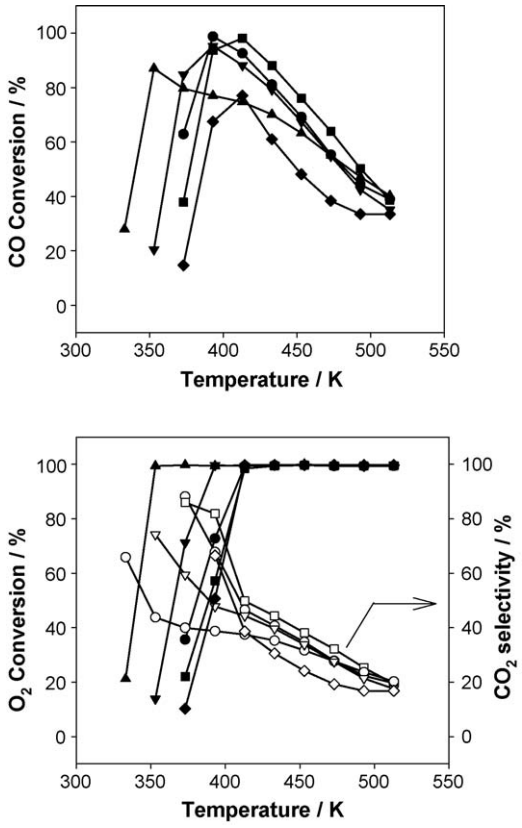

Fig. 3. CO conversion, O_2 conversion, and CO_2 selectivity for the PROX over modified CuO–CeO_2 with increasing reaction temperatures. CuO–CeO_2 (●, ○), HCl-added CuO–CeO_2 (■, □), 0.05% Pt(N)/CuO–CeO_2 (▲, △), 0.05% Pt(C)/CuO–CeO_2 (▼, ▽), and 0.05% Ru/CuO–CeO_2 (◆, ◇). Reactants: 1% CO, 1% O_2, 80% H_2, and 2% H_2O in He. F/W = 1000 ml/min/g_{cat}.

The effect of an additive to CuO–CeO_2 catalyst on the PROX was examined as shown in Fig. 3. The addition of Pt as a form of H_2PtCl_6 increased the CO conversion at a low temperature such as 373 K. The O_2 conversion also increased at low temperatures noticeably. Therefore, the CO_2 selectivity was lower over Pt(C)/CuO–CeO_2 catalyst for all reaction temperatures compared with that of CuO–CeO_2 catalyst. The low-temperature H_2 oxidation was further promoted when Pt was added to CuO–CeO_2 as a form of $Pt(NH_3)_4(NO_3)_2$. This caused much lower CO_2 selectivity at all reaction temperatures compared with that of CuO–CeO_2 catalyst. This lower CO_2 selectivity was also observed for Ru-, Ni-, and Co-promoted CuO–CeO_2 catalysts. The presence of chloride in CuO–CeO_2 lowered the catalytic activity for CO oxidation at low temperatures and just shifted the optimum temperature showing the highest CO conversion to a higher temperature. This adverse effect of chloride ion on the catalytic activity can be explained by the inhibition of redox cycle between copper oxide and ceria [10].

The PROX was examined over supported gold catalysts in the presence of 10% H_2 as shown in Fig. 4. Au/γ-Al_2O_3 showed 100% CO conversion when the reaction temperature was lower than 333 K. However, this CO conversion decreased rapidly as the reaction temperature increased further. Au/CuO showed 100% CO conversion when the reaction temperature was from 368 to 398 K. Au/CeO_2/γ-Al_2O_3 showed more than 90% CO conversion over a wide reaction temperature from 303 to 493 K. Au/CeO_2-DP also showed more than 95% CO conversions over a wide reaction temperature from 303 to 573 K. Hundred percent CO conversion was obtained over Au/CeO_2-CP at temperatures of 383–458 K. Au/CuO–CeO_2 showed more than 95% CO conversion at temperatures of 373–493 K. From this result in the presence of 10 vol.% H_2, Au/CeO_2-CP, Au/CeO_2-DP, and Au/CuO–CeO_2 were appeared to be active for the preferential CO oxidation and were chosen for the further study.

In the presence of 80% H_2, Au/CeO_2-CP showed the highest CO conversion at temperatures of 353–433 K as shown in Fig. 5. At high reaction temperatures such as above 533 K, Au/CeO_2-DP showed the higher CO conversion than did Au/CeO_2-CP. Au/CuO–CeO_2 was appeared to be the least selective for CO oxidation.

Table 1 shows the physical properties of supported gold catalysts examined in this study. The particle size of gold was smaller than 10 nm in all the gold catalysts. For supported gold catalysts, the catalytic activity was reported to be dependent on the detailed preparation procedure. The amount of residual chloride has also been claimed to be one of critical factors. However, it has been accepted that these factors finally affects

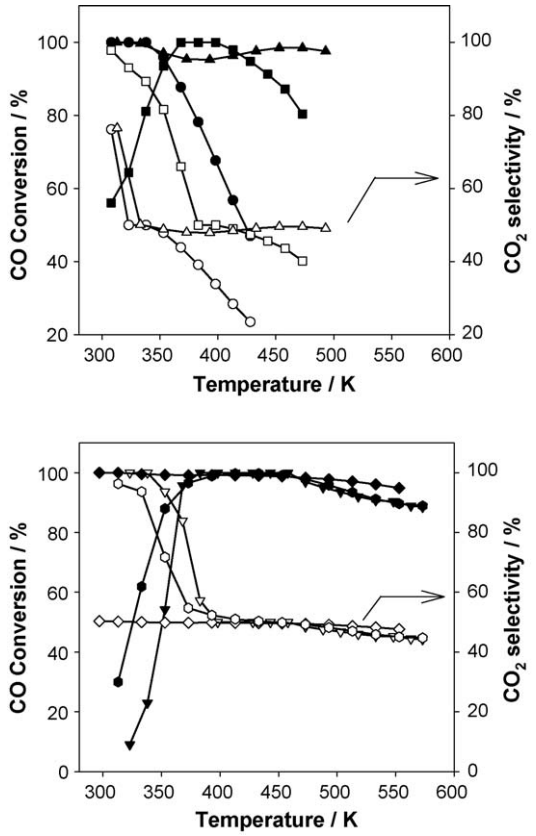

Fig. 4. CO conversion and CO_2 selectivity for the PROX over supported Au catalysts with increasing reaction temperatures. Catalysts: Au/γ-Al_2O_3 (●, ○), Au/CuO (■, □), Au/CeO_2/γ-Al_2O_3 (▲, △), Au/CeO_2-CP (▼, ▽), Au/CeO_2-DP (◆, ◇), and Au/CuO–CeO_2 (⬢, ⬡). Reactants: 1% CO, 1% O_2, 10% H_2, and 2% H_2O in He. F/W = 1000 ml/min/g_{cat}.

the particle size of gold which is closely related to the catalytic activity [52].

The catalytic activities of Pt/γ-Al_2O_3, Pt–Co/γ-Al_2O_3, and Pt–Ni/γ-Al_2O_3 were examined in the presence of 80% H_2 as shown in Fig. 6. Pt–Ni/γ-Al_2O_3 showed the highest CO conversion and CO_2 selectivity at temperatures of 373–453 K. The addition of Ni and Co increased the CO conversion and the

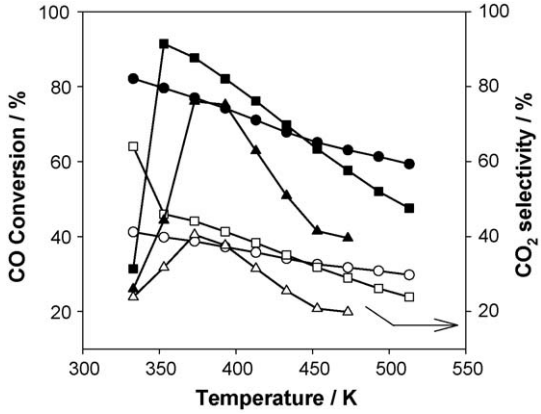

Fig. 5. CO conversion and CO_2 selectivity for the PROX over supported Au catalysts with increasing reaction temperatures. Au/CeO_2-DP (●, ○), Au/CeO_2-CP (■, □), and Au/CuO–CeO_2 (▲, △). Reactants: 1% CO, 1% O_2, 80% H_2, and 2% H_2O in He. F/W = 1000 ml/min/g_{cat}.

Table 1
Physical properties of supported gold catalysts

Catalyst	Au content (wt.%)[a]	BET surface area (m^2/g)	Au crystalline size (nm)[b]
Au/γ-Al_2O_3	0.48	170	5.6 ± 1.1
Au/CeO_2/γ-Al_2O_3	0.72	150	8.6 ± 1.7
Au/CuO	9.26	12	3.8 ± 0.5
Au/CuO–CeO_2	1.24	128	4.5 ± 1.0
Au/CeO_2-CP	0.95	113	4.7 ± 1.6
Au/CeO_2-DP	0.69	97	4.3 ± 1.0

[a] The amount of gold was determined by ICP.
[b] The particle size of Au was measured from TEM analysis.

CO_2 selectivity at low temperatures compared with those of Pt/γ-Al_2O_3 catalyst. The amount of chemisorbed CO on Pt/γ-Al_2O_3, Pt–Co/γ-Al_2O_3, and Pt–Ni/γ-Al_2O_3 was determined to be 34.8, 27.7, and 23.9 μmol/g_{cat}, respectively. This shows that the addition of cobalt and nickel decreased the amount of surface active site for CO chemisorption. The bulk crystalline structures were determined by XRD patterns. However, no peak corresponding to crystalline phase of platinum, nickel and cobalt compounds was found except peaks representing γ-Al_2O_3. Therefore, it can be assumed that these metals were present in a highly dispersed form, which was also supported by the CO chemisorption. This enhancement of catalytic activity was explained by the formation of bimetallic phase of Pt and Co (or Ni) in Pt–Co/γ-Al_2O_3, and Pt–Ni/γ-Al_2O_3, which was supported by the temperature programmed reduction (TPR) patterns [42,43].

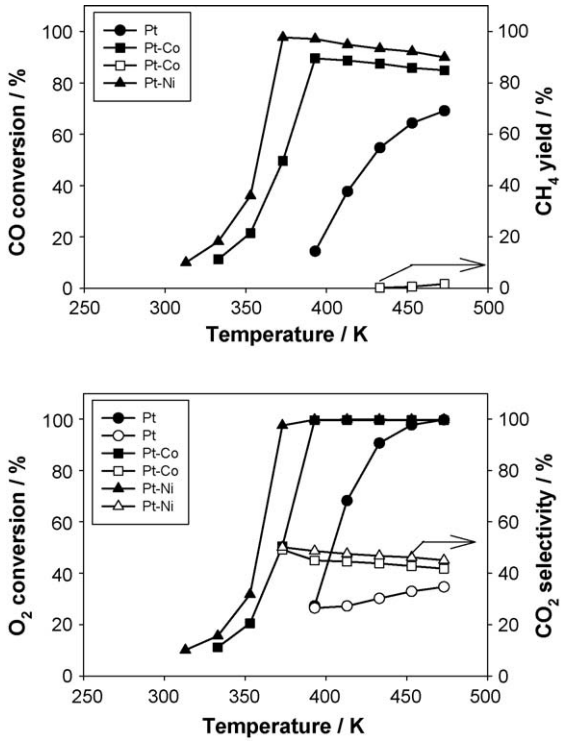

Fig. 6. CO conversion, CH_4 yield, O_2 conversion, and CO_2 selectivity for the selective CO oxidation over Pt/γ-Al_2O_3 (●, ○), Pt–Co/γ-Al_2O_3 (■, □), and Pt–Ni/γ-Al_2O_3 (▲, △) with increasing reaction temperatures. Reactants: 1% CO, 1% O_2, 80% H_2, and 2% H_2O in He. F/W = 1000 ml/min/g_{cat}.

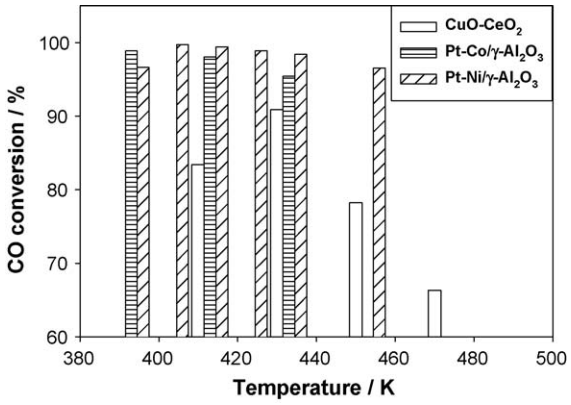

Fig. 7. CO conversion for the selective CO oxidation over $CuO–CeO_2$, Pt–Co/γ-Al_2O_3, and Pt–Ni/γ-Al_2O_3 at different reaction temperatures. Reactants: 1% CO, 1% O_2, 20% CO_2, 50% H_2, and 2% H_2O in He. F/W = 1000 ml/min/g_{cat}.

The effect of H_2O and CO_2 on the PROX was further examined over $CuO–CeO_2$ calcined in air at 373 K, Pt–Co/γ-Al_2O_3, and Pt–Ni/γ-Al_2O_3 catalyst as shown in Fig. 7. For all reaction temperatures, the higher CO conversion with a higher CO_2 selectivity was obtained over Co- or Ni-promoted Pt/γ-Al_2O_3 catalyst compared with that of $CuO–CeO_2$. Pt–Ni/γ-Al_2O_3 appeared to be superior to Pt–Co/γ-Al_2O_3 because the former had a wide reaction temperature range showing high CO conversions than the latter. 99.7% CO conversion was achieved over Pt–Ni/γ-Al_2O_3 catalyst at 403 K. The deactivation did not occur during 10 h reaction.

Finally, we compared catalytic performance of various PROX catalysts on the selective oxidation of CO under the same reaction condition. Pt–Ni/γ-Al_2O_3 seemed to be most effective catalyst for the PROX in the presence of excess H_2 in the reactant stream. This catalyst also showed the best performance in the presence of CO_2 and H_2O.

4. Conclusions

Pt–Ni/γ-Al_2O_3 showed high CO conversions over wide reaction temperatures for the PROX in the presence of excess H_2 among various PROX catalysts such as meal oxides such as CoO and $CuO–CeO_2$, supported gold catalysts such as Au/γ-Al_2O_3, Au/CuO, Au/CeO_2/γ-Al_2O_3, Au/$CuO–CeO_2$ and Au/CeO_2, and supported Pt catalysts such as Pt/γ-Al_2O_3, Pt–Ni/γ-Al_2O_3, and Pt–Co/γ-Al_2O_3. This Pt–Ni/γ-Al_2O_3 catalyst also showed the best performance in the presence of 2 vol.% H_2O and 20 vol.% CO_2.

Acknowledgement

We acknowledge financial support from the Samsung Advanced Institute of Technology (SAIT).

References

[1] C. Song, Catal. Today 77 (2002) 17.
[2] L. Shore, R.J. Farrauto, in: W. Vielstich, A. Lamm, H.A. Gasteiger (Eds.), Handbook of Fuel Cells: Fundamentals Technology and Applications, Part 2, vol. 3, John Wiley & Sons Ltd., West Sussex, 2003, p. 211.
[3] S. Wieland, T. Melin, in: W. Vielstich, A. Lamm, H.A. Gasteiger (Eds.), Handbook of Fuel Cells: Fundamentals Technology and Applications, Part 2, vol. 3, John Wiley & Sons Ltd., West Sussex, 2003, p. 202.
[4] S. Takenaka, T. Shimizu, K. Otsuka, Int. J. Hydrogen Energy 29 (2004) 1065.
[5] Y. Teng, H. Sakurai, A. Ueda, T. Kobaysahi, Int. J. Hydrogen Energy 24 (1999) 355.
[6] G. Avogouropolos, T. Ioannides, H.K. Matralis, J. Batista, S. Hocevar, Catal. Lett. 73 (2001) 33.
[7] J.B. Wang, W.-H. Shih, T.-J. Huang, Appl. Catal. A 203 (2000) 191.
[8] D.H. Kim, J.E. Cha, Catal. Lett. 86 (2003) 107.
[9] F. Marino, C. Descorme, D. Duprez, Appl. Catal. B 58 (2005) 175.
[10] G. Sedmak, S. Hocevar, J. Levec, J. Catal. 213 (2003) 135.
[11] G. Avogouropolos, T. Ioannides, H.K. Matralis, Appl. Catal. B 56 (2005) 87.
[12] G. Marban, A.B. Fuertes, Appl. Catal. B 57 (2005) 43.
[13] Y. Liu, Q. Fu, M.F. Stephanopoulos, Catal. Today 93–95 (2004) 241.
[14] C.R. Jung, J. Han, S.W. Nam, T.-H. Lim, S.-A. Hong, H.-I. Lee, Catal. Today 93–95 (2004) 183.
[15] M. Watanabe, H. Uchida, H. Igarashi, M. Suzuki, Chem. Lett. (1995) 21.
[16] J.B. Wang, S.-C. Lin, T.-J. Huang, Appl. Catal. A 232 (2002) 107.
[17] J.-W. Park, J.-H. Jeong, W.-L. Yoon, H. Jung, H.-T. Lee, D.-K. Lee, Y.-K. Park, Y.-W. Rhee, Appl. Catal. A 274 (2004) 25.
[18] J.W. Park, J.H. Jeong, W.L. Yoon, C.S. Kim, D.-K. Lee, Y.-K. Park, Y.W. Rhee, Int. J. Hydrogen Energy 30 (2005) 209.
[19] P. Ratnasamy, D. Srinivas, C.V.V. Satyanarayana, P. Manikandan, R.S. Senthil Kumaran, M. Sachin, V.N. Shetti, J. Catal. 221 (2004) 455.
[20] R. Lin, M.-F. Luo, Y.-J. Zhong, Z.-L. Yan, G.-Y. Liu, W.-P. Liu, Appl. Catal. A 255 (2003) 331.
[21] R.M.T. Sanchez, A. Ueda, K. Tanaka, M. Haruta, J. Catal. 168 (1997) 125.
[22] A. Luengnaruemitchai, D.T.K. Thoa, S. Osuwan, E. Gulari, Int. J. Hydrogen Energy 30 (2005) 981.
[23] M.J. Kahlich, H.A. Gasteiger, R.J. Behm, J. Catal. 182 (1999) 430.
[24] R.J.H. Grisel, C.J. Weststrate, A. Goossens, M.W.J. Craje, A.M. van der Kraan, B.E. Nieuwenhuys, Catal. Today 72 (2002) 123.
[25] R.J.H. Grisel, B.E. Nieuwenhuys, J. Catal. 199 (2001) 48.
[26] G. Panzera, V. Modafferi, S. Candamano, A. Donato, F. Frusteri, P.L. Antonucci, J. Power Sources 135 (2004) 251.
[27] W.-S. Shin, C.-R. Jung, J. Han, S.-W. Nam, T.-H. Lim, S.-A. Hong, H.-I. Lee, J. Ind. Eng. Chem. 10 (2004) 302.
[28] S. Carrettin, P. Concepcion, A. Corma, J.M.L. Nieto, V.F. Puntes, Angew. Chem. Int. Ed. 43 (2004) 2538.
[29] W. Deng, J.D. Jesus, H. Saltsburg, M. Flytzani-Stephanopoulos, Appl. Catal. A 291 (2005) 126.
[30] S.H. Oh, R.M. Sinkevitch, J. Catal. 142 (1993) 254.
[31] M. Echigo, T. Tabata, Catal. Today 90 (2004) 269.
[32] M. Echigo, T. Tabata, Appl. Catal. A 251 (2003) 157.
[33] R.A. Lemons, J. Power Sources 29 (1990) 251.
[34] H. Igarashi, H. Uchida, M. Suzuki, Y. Sasaki, M. Watanabe, Appl. Catal. A 159 (1997) 159.
[35] A. Manasilp, E. Gulari, Appl. Catal. B 37 (2002) 17.
[36] I.H. Son, M. Shamsuzzoha, A.M. Lane, J. Catal. 210 (2002) 460.
[37] O. Korotkikh, R. Farrauto, Catal. Today 62 (2000) 249.
[38] X. Liu, O. Korotkikh, R. Farrauto, Appl. Catal. A 226 (2002) 293.
[39] M. Watanabe, H. Uchida, K. Ohkubo, H. Igarashi, Appl. Catal. B 46 (2003) 595.
[40] A. Sirijaruphan, J.G. Goodwin Jr., R.W. Rice, J. Catal. 224 (2004) 304.
[41] I.H. Son, A.M. Lane, Catal. Lett. 76 (2001) 151.
[42] E.-Y. Ko, E.D. Park, K.W. Seo, H.C. Lee, D. Lee, S. Kim, Korean J. Chem. Eng. 23 (2006) 182.
[43] E.-Y. Ko, E.D. Park, K.W. Seo, H.C. Lee, D. Lee, S. Kim, J. Nanosci. Nanotechnol., in press.
[44] D.J. Suh, C. Kwak, J.-H. Kim, S.M. Kwon, T.-J. Park, J. Power Sources 142 (2005) 70.
[45] C. Kwak, T.-J. Park, D.J. Suh, Chem. Eng. Sci. 60 (2005) 1211.

[46] C. Kwak, T.-J. Park, D.J. Suh, Appl. Catal. A 278 (2005) 181.
[47] S.-H. Cho, J.-S. Park, S.-H. Choi, S.-H. Kim, J. Power Sources 156 (2006) 260.
[48] Y. Minemura, S. Ito, T. Miyao, S. Naito, K. Tomishige, K. Kunimori, Chem. Comm. (2005) 1429.
[49] C. Pedrero, T. Waku, E. Iglesia, J. Catal. 233 (2005) 242.
[50] G. Avgouropoulos, T. Ioannides, Ch. Papadopoulou, J. Batista, S. Hocevar, H.K. Matralis, Catal. Today 75 (2002) 157.
[51] T. Tabakova, F. Boccuzzi, M. Manzoli, J.W. Sobczak, V. Idakiev, D. Amdreeva, Appl. Catal. A 298 (2006) 127.
[52] H.-S. Oh, J.H. Yang, C.K. Costello, Y.M. Wang, S.R. Bare, H.H. Kung, M.C. Kung, J. Catal. 210 (2002) 375.